Influence of the heat treatment on the layer J_C of internal-Sn Nb_3Sn wires with internally oxidized nanoparticles

Lonardo, Francesco; Bovone, Gianmarco; Buta, Florin; Bonura, Marco; Bagni, Tommaso; Medina-Clavijo, B.; Ballarino, A.; Hopkins, S. C.; Boutboul, T.; Senatore, Carmine

How to cite

LONARDO, Francesco et al. Influence of the heat treatment on the layer J_C of internal-Sn Nb_3Sn wires with internally oxidized nanoparticles. In: IEEE transactions on applied superconductivity, 2024, vol. 34, n° 5, p. 6000305. doi: 10.1109/TASC.2024.3355353

This publication URL: https://archive-ouverte.unige.ch/unige:174381

Publication DOI: 10.1109/TASC.2024.3355353

5OrM2-6

Influence of the heat treatment on the layer J_C of internal-Sn Nb_3Sn wires with internally oxidized nanoparticles

F. Lonardo, G. Bovone, F. Buta, M. Bonura, T. Bagni, B. Medina-Clavijo, A. Ballarino, S. C. Hopkins, T. Boutboul and C. Senatore

***Abstract*—We evaluated various heat treatments (HT) for maximizing the Nb_3Sn layer thickness while retaining a refined grain microstructure in low filament count internal-Sn Nb_3Sn Rod-In-Tube wires with internally oxidized nanoparticles. These wires were manufactured in our laboratory using SnO_2 as oxygen source and Nb alloys containing Ta and Zr or Hf. By reacting the wires at 650°C for 200 hours we obtained relatively thin reaction layers but high layer critical current densities (layer J_C) of ~3000 A/mm² for Hf-containing wires and ~2700 A/mm² for Zr-containing wires, both at 4.2 K and 16 T. Notably, both of these values are over the layer J_C threshold of 2500 A/mm², which is estimated to be necessary for attaining the corresponding Future Circular Collider (FCC) target non-Cu J_C of 1500 A/mm². Following this heat treatment, the fine-grained Nb_3Sn area occupies only ~35% of the filament area for Hf-containing wires and ~20% for Zr-containing wires. After heat treatments with a reaction step at 700°C these values increase to 70-80% and ~60%, respectively, with only a minor increase of the grain size. However, we observed a noticeable decrease in the layer J_C for these HT. Magnetic measurements show that the high J_C wires exhibit a point defect contribution from precipitates to the pinning force, which is missing in wires with depressed J_C values. The higher heat treatment temperatures may have caused excessive coarsening of the oxide precipitates, to sizes unsuitable for flux pinning. Reaction heat treatment temperatures in the range of 650°C to 700°C and durations between 50 and 200 hours may provide a better compromise between the Nb_3Sn layer thickness, its grain size and nanoparticle size.**

***Index Terms*—** Nb_3Sn, Internal Oxidation, Heat Treatment, Superconducting Wire, Pinning Force.

Submitted for review September 26, 2023

This work was performed under the auspices from the Swiss Accelerator Research and Technology (CHART) program, https://chart.ch. Financial support was provided by the Swiss National Science Foundation (Grant No. 200021_184940) and by the European Organization for Nuclear Research (CERN), Memorandum of Understanding for the FCC Study, Addendum FCC-GOV-CC-0175 (KE4663/ATS). The authors are also grateful to Damien Zurmuehle for all his help with the laboratory work and the experiments.

F. Lonardo, G. Bovone, F. Buta and M. Bonura are with the Department of Quantum Matter Physics, University of Geneva, Geneva, Switzerland. F. Lonardo can be contacted by e-mail at francesco.lonardo@unige.ch.

T. Bagni was with the Department of Quantum Matter Physics, University of Geneva, Geneva, Switzerland. He is now with the Department of Physics and Astronomy, FREIA, Uppsala University, Uppsala, Sweden.

B. Medina-Clavijo, A. Balarino, S. C. Hopkins and T. Boutboul are with the European Organization for Nuclear Research, CERN, Geneva, Switzerland.

C. Senatore is with the Department of Quantum Matter Physics and the Department of Nuclear and Particle Physics, University of Geneva, Geneva, Switzerland (e-mail: carmine.senatore@unige.ch).

I. INTRODUCTION

THE Future Circular Collider (FCC-hh), a new proton-proton collider proposed by the European Organization for Nuclear Research (CERN), is aimed to reach a collision energy of 100 TeV [1]. This goal would be achievable with a 100-kilometer circumference ring, incorporating a powerful 16 T Nb_3Sn dipole magnet system. To keep the project economically and technically feasible, dipole magnets must be compact, which needs higher non-Cu J_C (critical current, I_C, per non-Cu area, the cross-sectional area of the wire excluding the Cu stabilizer) of the superconducting wires. Taking as a reference the design of the Nb_3Sn wires developed for the HL-LHC upgrade, the FCC target of 1500 A/mm² for the non-Cu J_C, at 4.2K and 16T, corresponds to a layer J_C (i.e. I_C divided by the Nb_3Sn area) of 2500 A/mm² [2]. Such a high layer J_C in Nb_3Sn wires can be achieved by refining the grains of the superconducting material with the so-called internal oxidation process [3]. This process adds an oxygen source (OS) to the wire layout and a high oxygen-affinity element to the Nb alloy. The internal oxidation of the latter forms oxide nanoparticles that lead to a reduced final Nb_3Sn mean grain size (G_{mean}). Both grain refinement and artificial pinning centers (oxide nanoparticles) contribute to enhance the total pinning force density ($f_P = J_C \times B$) and consequently the layer J_C [3]. In the framework of a collaboration between the University of Geneva and CERN, we recently fabricated simplified Rod-In-Tube (RIT) wires implementing the internal oxidation process, using Hf− and Zr− containing alloys [4]. This enabled us to explore the effects of the OS position relative to the Nb_3Sn formation front. With a heat treatment (HT) at 650°C for 200 hours, we achieved a G_{mean} of Nb_3Sn of 50 nm for Hf−containing and 60 nm for Zr−containing samples. The layer J_C values for these samples were 3000 and 2700 A/mm² respectively at 4.2 K and 16 T, both exceeding the layer J_C target of 2500 A/mm². We noticed significantly lower Nb_3Sn layer thicknesses in wires containing internally oxidized nanoparticles than in wires based on the same alloys but without an OS. In view of implementing internal oxidation in high filament count subelements to be used for application-ready wires, we performed an HT optimization study. The goal is to increase the reaction layer thickness (d_L) (in other word to enhance its growth kinetics) without causing excessive grain growth. This paper reports on the effect of different heat

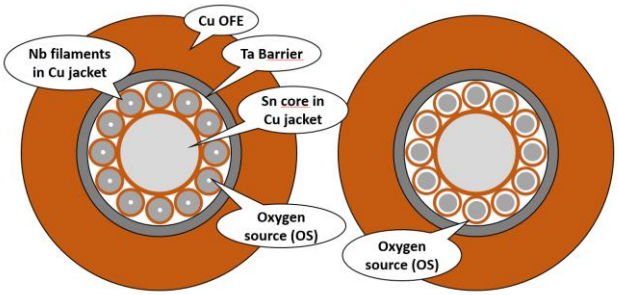

Fig. 1. Rod-in-tube design. On the left, the coreOS configuration, in which the white dot in the center of each filament is the OS. On the right, the annularOS configuration in which the OS is represented as a white ring between the Nb-alloy and the Cu jacket of each filament.

TABLE I
LIST OF THE EXAMINED WIRES

Wire Type ID	*Nb-alloy (wt%)*	*Oxygen Source position*
Hf-annularOS	Nb-7.5%Ta-2%Hf	Annular
Zr-annularOS	Nb-7.5%Ta-1%Zr	Annular
Zr-coreOS	Nb-7.5%Ta-1%Zr	Core

treatment (HT) parameters, such as temperature (T) and duration of the treatment (t), on the d_L, G_{mean}, transport properties, and pinning mechanism of our wires.

II. EXPERIMENTAL

A. Samples

The wires, whose layouts are shown in figure 1, are made of 12 Nb-alloy filaments in a Cu jacket arranged around a central Cu-clad Sn rod, the whole assembly being enclosed in a tantalum tube. This Ta barrier is essential to prevent the contamination with Sn of the external stabilizer copper during the HT. Two alloys – Nb−7.5wt%Ta−2wt%Hf and Nb−7.5wt%Ta−1wt%Zr – were used to compare the effect of internal oxidation and HT on the properties of Nb_3Sn. They were employed in two OS layouts: coreOS, with the OS in the core of each Nb-alloy filament, and annularOS, where the OS lies at the periphery of each filament, between the Nb-alloy and the Cu jacket. More details regarding the layout, composition and manufacturing can be found in [4]. A list of the manufactured wires is reported in Table I.

B. Heat treatment

The HT was conducted under vacuum or under Ar (in sealed quartz tubes) and was made of two distinct plateaus. The 1st plateau at 550°C for 100 hours, reached with a ramp rate of 50°C/hour, used also in [7], was proposed to facilitate the diffusion of oxygen into the Nb alloy prior to the formation of Nb_3Sn. During the 2nd plateau, reached with the same ramp rate, the Nb_3Sn phase forms and grows. We systematically varied the Temperature-time (T-t) of the 2nd plateau to investigate the influence of the two parameters on the reaction layer and grain size. To minimize the number of samples to be analysed we have first run a series of heat treatments with a wide range of

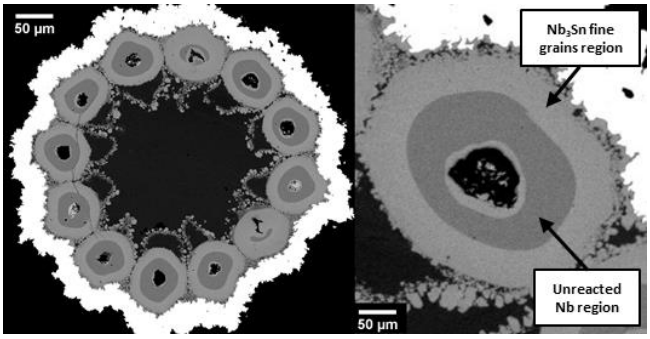

Fig. 2. On the left, the back-scattered electron SEM image of a polished cross-section for a Zr-coreOS wire heat treated at 700°C×50h. On the right, a single filament of the same cross-section. The central unreacted Nb-alloy is surrounded by the fine grains Nb_3Sn layer and then the large grains of Nb_3Sn and other phases.

temperatures and durations (Table II) but limited to the Hf-annularOS samples. Based on the results of this series we have then selected the heat treatments that were applied to the rest of the wire types (Table III and Table IV).

C. Characterization techniques

The size of the Nb_3Sn grains was determined by employing the line intercept method on electron micrographs of fractured cross-sections. Consistent with our previous research [4], [8], wires with an OS exhibited slightly elongated Nb_3Sn grains. Hence, we evaluated the grain size in both the long-axis (G_L) and short-axis (G_S) directions by measuring the intercept distances of two lines for each axis, in each analysed image. These two dimensions were then used to calculate G_{mean} as an arithmetic mean. Multiple images (ranging from 5 to 10) were analysed for each wire sample to calculate the mean intercept distance (arithmetic mean), along with its standard deviation. Figure 2 displays an image of a polished cross-section of a Zr-coreOS wire captured using back-scattered electrons in a field emission scanning electron microscope (FESEM). To quantify the fraction of the fine grain reaction layer, we use the ratio $r_{fine\ grain}$, defined as the area of the fine grain region divided by the area of the fine grain region plus the area enclosed that includes the unreacted residual Nb-alloy. The I_C measurements were carried out at 4.2 K in magnetic fields up to 19 T at the University of Geneva. The samples, 46 mm in length, were provided with two sets of voltage taps placed at distances of approximately 20 mm and 10 mm. A criterion of 0.1 µV cm^{-1} was employed. The layer J_C was calculated by dividing I_C by the fine grain area determined on actual cross-sectional samples taken from the measured wire segment. The estimation excludes the coarse grains of Nb_3Sn because their transport properties are negligible [9]. Magnetic measurements were performed in a temperature range from 4.2 K to 16 K using a VSM-SQUID magnetometer installed at the University of Geneva and a VSM magnetometer from Cryogenic Ltd installed at CERN, with magnetic fields up to 7 T and 10.5 T, respectively. The M(H) loops acquired were used to calculate the pinning force density and investigate the pinning mechanism.

TABLE II

HF-ANNULAROS: LIST OF $R_{FINE\ GRAIN}$, LONG AXIS GRAIN SIZE (G_L), SHORT AXIS GRAIN SIZE(G_S), LAYER J_C, AND B/B_K OF THE PINNING FORCE DENSITY PEAK FOR DIFFERENT HT

Zr-coreOS								
T – t [1st plateau]		T – t [2nd plateau]		$r_{fine\ grain}$	G_L	G_S	layer J_C (16T, 4.2K)	B/B_k
°C	hours	°C	hours	%	[nm]	[nm]	[A/mm^2]	
550	100	650	100	31 ± 6	62 ± 5	40 ± 3	n.a. [1]	n.a.
550	100	650	200	35 ± 4	62 ± 3	42 ± 5	3030 [4]	0.3[2]
550	100	650	300	48 ± 4	61 ± 4	46 ± 2	n.a.	0.3[2][4]
550	100	675	200	63 ± 5	70 ± 5	48 ± 3	n.a.	0.25[3][4]
550	100	700	50	42 ± 3	65 ± 5	47 ± 4	1930	0.2[2]
550	100	700	100	56 ± 2	68 ± 6	48 ± 2	1880	0.2[2]
550	100	700	200	73 ± 7	75 ± 6	49 ± 2	n.a.	n.a.
550	100	700	300	80 ± 6	90 ± 13	50 ± 2	n.a.	n.a.
550	100	750	50	67 ±2	174 ± 17	75 ± 7	n.a.	n.a.
550	100	750	100	74 + 2	203 ± 28	82 ± 1	n.a.	n.a.

[1]n.a.: the value of the layer J_C is not measured either because the sample or HT does not meet the criteria, or because the measurements have not yet been performed.
[2]Measured with VSM-SQUID magnetometer at University of Geneva.
[3]Measured with VSM magnetometer of Cryogenic Ltd at CERN.
[4]Data not shown.

III. RESULTS AND DISCUSSION

A. *Results of the screening analysis to determine the most promising heat treatments.*

Table II contains the G_L, G_S, $r_{fine\ grain}$, layer J_C, and the reduced field corresponding to the pinning force density peak of Hf-annularOS samples, which is the wire type used to identify the most promising heat treatments. We analysed these results looking for an increase of $r_{fine\ grain}$ and limited growth of G_{mean} (less than 10%), in order to preserve an average grain size close to that of the high-Jc samples heat treated at 650°C×200 h. Another factor that guided the selection was our preference for HT durations below 200 h that are more practical/economical for full scale magnets [10]. We identified three suitable HT: 700°C×50 h, 700°C×100 h, and 675°C×200 h. We have not yet carried out transport measurements on the samples heat treated at 675°C for 200 h but we will discuss later its prospects. Figure 3 shows G_{mean} and $r_{fine\ grain}$ as function of the duration for the different HT temperatures of this screening analysis. Previous works [10], [11], [12], and [13] reported a power law (t^{β}) dependence of the grain growth and fine grain area as a function of time, with exponents β of 0.11 and 0.36, respectively. We observe that in this range of temperatures and durations the mean grain size depends strongly on the HT temperature but only weakly on the HT duration. The fitting performed on the data obtained for the Hf-annularOS wires treated at 650°C and 700°C produced similar results for β, 0.10 for grain growth and 0.36 for fine grain area. As only two points are available at 750°C we have generated a predictive curve of growth using the exponents determined at the other temperatures. Samples reacted at 750°C show an excessive grain growth, exceeding our chosen limit for G_{mean}.

TABLE III

ZR-COREOS: LIST OF $R_{FINE\ GRAIN}$, LONG AXIS GRAIN SIZE (G_L), SHORT AXIS GRAIN SIZE(G_S), LAYER J_C, AND B/B_K OF THE PINNING FORCE DENSITY PEAK FOR DIFFERENT HT

Zr-coreOS								
T – t [1st plateau]		T – t [2nd plateau]		$r_{fine\ grain}$	G_L	G_S	layer J_C (16T, 4.2K)	B/B_k
°C	hours	°C	hours	%	[nm]	[nm]	[A/mm^2]	
550	100	650	200	22 ± 2	72 ± 12	52 ± 9	2710 [4]	0.27[2]
550	100	675	200	70 ± 12	75 ± 7	54 ± 3	n.a.	n.a
550	100	700	50	57 ± 11	73 ± 5	53 ± 2	2220	0.2[2]
550	100	700	100	58 ± 6	83 ± 8	54 ± 4	2130	0.2[2]

[2]See note following Table II

TABLE IV

ZR-ANNULAROS: LIST OF $R_{FINE\ GRAIN}$, LONG AXIS GRAIN SIZE (G_L), SHORT AXIS GRAIN SIZE(G_S), LAYER J_C, AND B/B_K OF THE PINNING FORCE DENSITY PEAK FOR DIFFERENT HT

Zr-annularOS								
T – t [1st plateau]		T – t [2nd plateau]		$r_{fine\ grain}$	G_L	G_S	layer J_C (16T, 4.2K)	B/B_k
°C	hours	°C	hours	%	[nm]	[nm]	[A/mm^2]	
550	100	650	200	18 ± 2	78 ± 6	57 ± 5	2630 [4]	0.24[2]
550	100	675	200	55 ± 4	84 ± 5	55 ± 3	n.a.	0.2[3][4]
550	100	700	100	30 ± 11	80 ± 4	65 ± 6	1220	0.2[2]

[2,3,4]See note following Table II

B. *Evaluation of the selected heat treatments on all the wire types*

The values of G_L, G_S, $r_{fine\ grain}$, layer J_C, and the reduced field corresponding to the pinning force density peak of for the Zr-coreOS and Zr-annularOS wires are reported in the Tables III and IV, respectively. These samples follow the same behaviour as the Hf-annularOS ones. The values of G_{mean} of the Hf-annularOS, Zr-annularOS, and Zr-coreOS samples reacted at 700°C increase by about 10%, remaining close to the values of the samples reacted at 650°C. However, we observe a decrease of the layer J_C by 20-30% for the Hf-annularOS and Zr-coreOS samples reacted at 700°C with respect to the same wire types heat-treated at 650°C for 200h. For the Zr-annularOS sample the layer J_C is decreased by about 60% but its G_{mean} is comparable to the values of our samples heat-treated at 650°C. As the grain refinement and, thus, the grain boundary density is preserved, and the stoichiometry is not affected by different heat treatments, we argue that there has been a modification in the pinning contribution from the nanoparticles, which plays a role in the reduction of J_C. In ref. [14], it is reported that in the case of a PIT wire the loss of the contribution of artificial pinning centres decreased the total pinning force by 45–50% in magnetic fields of 15 to 20 T. We performed an analysis of the pinning force curves obtained combining magnetization measurements and transport current data to shed light on the observed reduction of J_C. As shown in figure 4 and listed in Tables II, III and IV, all samples heat-treated at 700°C show a maximum of the normalized pinning force density (F_P/F_P (max)) at 0.2 of the reduced field (B/B_K), which is usually related to a pure grain boundary pinning mechanism [15]. F_P/F_P (max) of Zr-coreOS, Zr-annularOS and Hf-annularOS samples heat-treated at 650°C for 200 h fall at 0.24, 0.27 and 0.3, respectively [4]. The shift to a higher reduced field is attributed

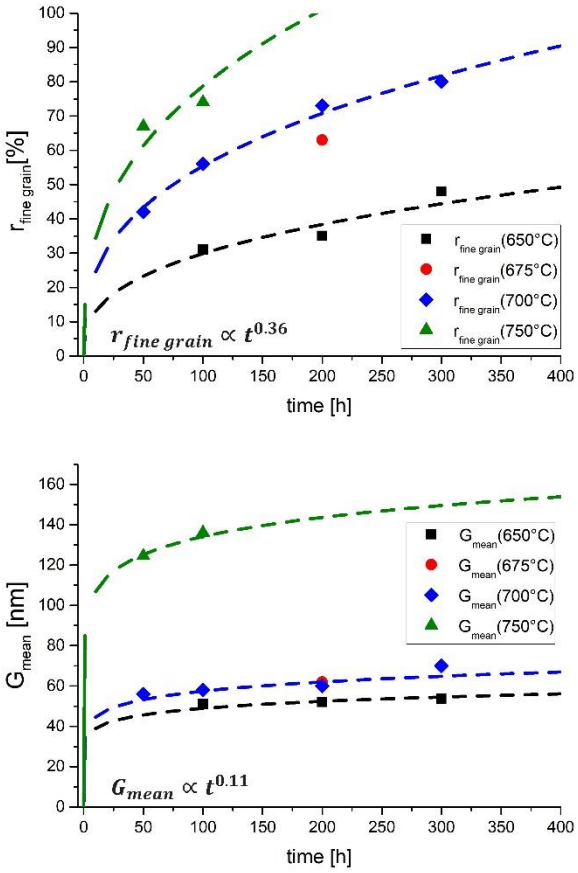

Fig. 3. The top graph shows the values (square symbols) and fitting curves (dash lines) of $r_{fine\ grain}$ for the Hf-annularOS samples as a function of the HT time. The bottom graph shows the values (square symbols) and fitting curve (dash lines) of G_{mean} for the Hf-annularOS samples as a function of the HT time.

to the presence of two pinning site types: grain boundary pinning, characterized by a maximum at $B/B_K = 0.20$ (with $B_K = B_{Kramer}$) and point defects pinning with the maximum at $B/B_K = 0.33$ [14]. Similar effects are present even at lower HT temperatures when the duration is particularly long, but they depend on the type of nanoparticles. The Hf-annularOS sample heat treated at 650°C for 300 hours still showed the peak at B/B_K =0.3, while for the Zr-coreOS and Zr-annularOS wires it was at 0.22 and 0.20, respectively. This underlines the important role of T-t in the growth of the oxide nanoparticle size, as already pointed out in [16], [17], [18]. We infer that the higher temperature and, to a lower extent in the explored range, the duration of the heat treatment has induced a coarsening of the oxide nanoparticles and thus reduced their ability to act as point defects to pin the fluxons. We lack a direct metallographic confirmation that the HT at 700°C causes nanoprecipitates to grow to such a size that the point defect pinning is not possible, but we plan to do systematic nanoparticle size studies in the future. The $r_{fine\ grain}$ values of samples heat treated at 675°C×200h are higher than those of the samples heat treated

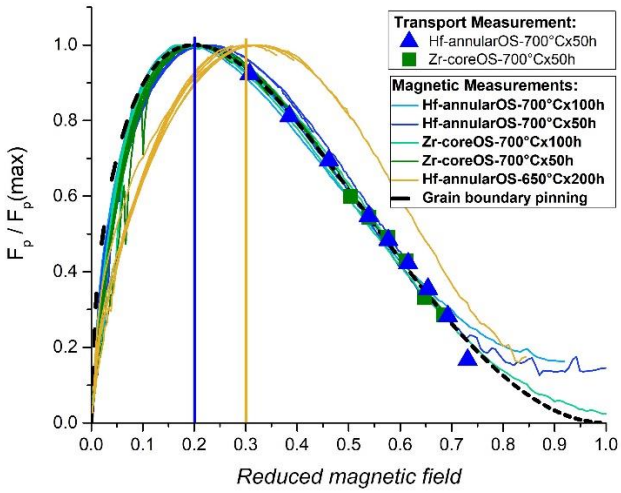

Fig. 4. Normalized pinning Force (F_P/F_P (max)) as function of the reduced field (B/B_K) of all the samples in tables II, III and IV heat-treated at 550°C×100h + 700°C×500h, 550°C×100h + 700°C×100h.The magnetic measurements have been acquired in the temperature range from 4.2 to 16 K and in magnetic fields up to 7 T.

at 700°C×100h: in Zr-coreOS samples it is 70% instead of 58%, while in Hf-annularOS samples it is 63% instead of 56%. Additionally, the values of G_{mean} are reduced for the Zr-coreOS sample (62 nm instead of 70 nm) but remain unchanged for the Hf-annularOS sample. Regarding the magnetic measurements, we have observed a partial loss of the APC contribution with a shift to 0.25 of the peaks of F_P for the Hf-annular wire and a complete loss of APC contribution for the Zr-annular samples. We infer that the plateau temperature at 675°C resulted in coarsening of the nanoparticles, which is less pronounced compared to the heat treatment with a plateau at 700°C. On the other hand, for the Zr-annularOS sample, that shows a lower contribution to pinning from oxide nanoparticles at 650°C, the implementation of heat treatments at higher temperatures are clearly detrimental. For the Hf-based samples, we can still consider 675°C as an alternative heat treatment temperature, with a reduced time to increase $r_{fine\ grain}$ and reduce the detrimental effect on the APC contribution to pinning. For the Zr-based wire, we can only consider lower temperatures and/or durations than 650°C × 200h to enhance or maintain the APC contribution. Such lower temperature heat treatments are also of interest for rod-in-tube wires with internally oxidized particles with finer filaments and will become a subject of study as soon as wires of this type become available.

IV. CONCLUSION

This article presents the results of experiments conducted to explore how different HT parameters influence the J_C of low filament count internal-Sn Rod-In-Tube Nb_3Sn wires with internally oxidized nanoparticles. In a previous work [4] we found out that the heat treatment at 650°C for 200 hours resulted in a layer J_C above the FCC target with a mean grain size in the

range of 50 nm and 70 nm. By changing the HT parameters (temperature and duration of the last plateau), we successfully increased the fine grain size area by about 10%, 20%, and 35% for Zr-annularOS, Hf-annularOS, and Zr-coreOS, respectively. The higher temperature enlarged the grains of all samples by a maximum of 10% compared to the samples heat-treated at 650°C for 200 hours. Despite the limited grain growth, the layer J_C decreases from over 3000 A/mm^2 down to 1900 A/mm^2 for Hf-annularOS wire, from 2700 A/mm^2 to 2200 A/mm^2 for Zr-coreOS wire, and from 2600 A/mm^2 to 1220 A/mm^2 for Zr-annularOS. The decrease of the layer J_C is more than expected from the modest increase of the grain size and can be related to a change in the relative weight of pinning contributions from grain boundaries and nanoparticles. The Hf-annularOS sample reacted at 650°C for 200 hours exhibits the maximum of the pinning force shifted to the value of reduced field $B/B_K = 0.3$. This is due to the contribution to pinning from oxide nanoparticles (point defect mechanism), a mechanism that seems not to be present in the samples heat treated at 700°C, where the peak is at $B/B_K = 0.2$, as in the case of pure grain boundary pinning. We infer that the reason for the absence of the point defect mechanism in the samples reacted at 700°C is excessive growth of the oxide nanoparticles, beyond the size that makes them suitable for fluxon pinning. Measurements of the size and number concentration of these nanoparticles are not available at this stage, but we plan an additional study of the size of nanoparticles in the future. Overall, the study demonstrates the importance of heat treatments in optimizing the superconducting properties of Nb_3Sn wires for high-field magnet applications. Further research will explore the effects of other heat treatments between 650°C and 700°C to identify an optimal balance between retaining point defect pinning and maximizing layer growth rate. Temperature below 650°C are not of interest to us at this stage of the wire development since they require longer HT times, which we aim to avoid.

REFERENCES

[1] Abada et al, “FCC-hh: The Hadron Collider”. Eur. Phys. J. Spec. Top. 228, 755–1107 (2019).

[2] Apollinari G et al, “High-luminosity Large Hadron Collider (HL-LHC)” (https://doi.org/ 10.23731/CYRM-2017-004)

[3] X. Xu, M. Sumption, X. Peng, and E. Collings, “Refinement of Nb_3Sn grain size by the generation of ZrO_2 precipitates in Nn_3Sn wires”, Applied physics letters 104(8) (2014)

[4] G. Bovone, F. Buta, F. Lonardo, T. Bagni, M. Bonura, D. LeBeouf, S. C. Hopkins, T. Boutboul, A. Ballarino, C. Senatore, “Effects of the oxygen source configuration on the superconducting properties of internally oxidized internal-Sn Nb_3Sn wires”, Superconductor Science and Technology, http://iopscience.iop.org/article/10.1088/1361-6668/aced25, 2023

[5] I. Weber, E. Longo, and E. Leite, “$SnO_2{\cdot}Nb_2O_5$ films for ethanol sensor, obtained by deposition of alcoholic suspensions”, Materials Letters 43(4), 166 (2000).

[6] D. Landolt, “Fundamental aspects of electropolishing”, Electrochemical Acta 32(1), 1 (1987).

[7] S. Balachandran, C. Tarantini, P. J. Lee, F. Kametani, Y.-F. Su, B. Walker, W. L. Starch, and D. C. Larbalestier, “Beneficial influence of hf and Zr additions to Nb4at%Ta on the vortex pinning of Nb_3Sn with and without an O source”, Superconductor Science and Technology 32(4), 044006 (2019).

[8] F. Buta, M. Bonura, D. Matera, G. Bovone, A. Ballarino, S. Hopkins, B. Bordini, X. Chaud, and C. Senatore, “Very high upper critical fields and enhanced critical current densities in Nb_3Sn superconductors based on Nb–Ta–Zr alloys and internal oxidation”, Journal of Physics: Materials 4(2), 025003 (2021)

[9] R. Flükiger, D. Uglietti, C. Senatore, F. Buta, Microstructure, composition and critical current density of superconducting Nb3Sn wires, Cryogenics, Volume 48, Issues 7–8, 2008, Pages 293-307

[10]ISSN 0011-2275H. Muller and T. Schneider, “Heat treatment of Nb_3Sn conductors”, Cryogenics 48(7-8), 323 (2008)

[11]H. Farrell, G. Gilmer, and M. Suenaga, “Grain boundary diffusion and growth of intermetallic layers: Nb_3Sn”, Journal of Applied Physics 45(9), 4025 (1974)

[12]CF. Old and I. Macphall, “Th mechanism and kinetics of growth of the superconducting compound Nb_3Sn”, Journal of Materials Science 4, 202 (1969)

[13]K. OSAMURA, S. OCHIAI, and T. UEHARA, “Mechanical and superconducting properties of multifilamentary Nb_3Sn composites”, Memoirs of the Faculty of Engineering, Kyoto University 51(3), 187 (1989)

[14]Jacob Rochester, “The Roles of Grain Boundary Refinement and Nano-Precipitates in Flux Pinning of APC Nb_3Sn”, IEEE TRANSACTIONS ON APPLIED SUPERCONDUCTIVITY, VOL. 31, NO. 5, AUGUST 2021

[15]Dew-Hughes, “Flux pinning mechanisms in type II superconductors”, The Philosophical Magazine: A Journal of Theoretical Experimental and Applied Physics, 1974).

[16]Xu X, Peng X, Rochester J, Lee J and Sumption M 2020 “High critical current density in internally oxidized Nb_3Sn superconductors and its origin” Scr. Mater.

[17]X. Xu, X. Peng, J. Rochester, M. Sumption, J. Lee, G. Calderon Ortiz, and J. Hwang, “The strong influence of Ti, Zr, Hf solutes and their oxidation on microstructure and performance of Nb_3Sn superconductors”, Journal of Alloys and Compounds 857, 158270 (2021).

[18]J. Lee, Z. Mao, D. Isheim, D. N. Seidman, and X. Xu, “Un-veiling the nucleation and growth of Zr oxide precipitates of internally oxidized Nb_3Sn superconductors”, arXiv preprint arXiv:2306.10866 (2023).